Talanta 197 (2019) 356–362

Contents lists available at ScienceDirect

Talanta

journal homepage: www.elsevier.com/locate/talanta

Direct, selective and ultrasensitive electrochemical biosensing of methyl parathion in vegetables using *Burkholderia cepacia* lipase@MOF nanofibers-based biosensor

Zhipan Wang[a], Baokai Ma[b], Cai Shen[b], Ling-Zhi Cheong[a,*]

[a] Department of Food Science and Engineering, College of Food and Pharmaceutical Sciences, Ningbo University, Ningbo 315211, China
[b] Institute of Materials Technology & Engineering, Chinese Academy of Sciences, 1219 Zhongguan Road, Ningbo 315201, China

ARTICLE INFO

Keywords:
Lipase Metal organic framework
Electrochemical properties Biosensor
Organophosphorus pesticides

ABSTRACT

Methyl parathion is one of the most widely used pesticides in agricultural practices. It caused accumulation of acetylcholine and over-stimulation of receptors in synapses which eventually led to damage of the nervous system. Present study developed a direct, sensitive, rapid and reliable method for methyl parathion residues detection in vegetable samples. MOF nanofibers which demonstrated stable framework structure, good thermal/chemical stability, good electrochemical behavior, high porosity, surface area and pore volume was synthesized and used for fabrication of *Burkholderia cepacia* lipase (BCL)@MOF nanofibers biosensors. BCL@MOF nanofibers/chitosan/GCE biosensor demonstrated high sensitivity for methyl detection with a wide linear range (0.1–38 μM) and low limit of detection 0.067 μM. During the 3 weeks storage stability test at 4 °C, the fabricated biosensor demonstrated good reusability and excellent stability for methyl parathion detection with retainment of more than 80% of its initial response. When applied for detection of methyl parathion residues in vegetable samples, the BCL@MOF nanofibers/chitosan/GCE biosensors demonstrated good recovery rates.

1. Introduction

Pesticides are globally used to control a range of pests infesting agricultural crops [1]. Methyl parathion is one of the most widely used pesticides in agricultural practices. It is relatively insoluble in water, poorly soluble in petroleum ether and mineral oils, and readily soluble in most organic solvents [2]. Methyl parathion are found to inhibit enzymes in the neurosynapses which resulted in accumulation of acetylcholine, over-stimulation of receptors in synapses and eventually led to damage of the nervous system [3]. Thus, there is a need to develop a direct, sensitive, rapid and reliable method for methyl parathion residues detection in food.

At present, several analytical methods are used to detect methyl parathion residues including gas chromatography and high performance liquid chromatography coupled to sensitive and specific detectors such as nitrogen-phosphorous detectors, flame ionization detectors, ultraviolet detectors, diode array detector and mass spectrometry [4–7]. These methods are complex, time-consuming, require the use of highly trained personnel and are not convenient for on-site analysis.

Biosensors particularly enzyme-based electrochemical biosensors have become a viable, handy, popular and potentially portable tool for detecting a wide spectrum of analytes including organophosphate pesticides such as methyl parathion [8–13]. Some of the enzymes used in electrochemical biosensing of methyl parathion include acetylcholinesterase [14], butyryl cholinesterase, organophosphorus acid anhydrolase and organophosphorus hydrolase [4]. These enzymes are either pricey, not commercially available or require complex purification steps.

Lipases (triacylglycerol ester hydrolases, EC 3.1.1.3) which catalyzes hydrolysis and synthesis of long-chain acylglycerols and many other esters in aqueous/organic biphasic media, are one of the most widely used biocatalysts in organic chemistry [15–17]. Unlike aforementioned enzymes such as acetylcholinesterase and organophosphorus hydrolase, lipases are commercially available at affordable price. This has made lipase-based electrochemical biosensors an attractive option for methyl parathion detection [18]. Lipases have only recently been used in electrochemical biosensor for detection of organophosphate pesticides including methyl parathion [8,10,19–22]. Some of the reported lipase-based biosensor is enzyme-inhibition-biosensor which operates by measuring percent inhibition of lipase activity due to exposure to methyl parathion [12,23–25].

Performance of enzyme electrochemical biosensors particularly

* Corresponding author.
E-mail address: lingzhicheong@yahoo.com (L.-Z. Cheong).

https://doi.org/10.1016/j.talanta.2019.01.052
Received 12 September 2018; Received in revised form 10 January 2019; Accepted 13 January 2019
Available online 14 January 2019
0039-9140/ © 2019 Elsevier B.V. All rights reserved.

sensitivity and reusability depends largely on immobilization of enzymes on electrode [26,27]. Recently, metal-organic frameworks (MOFs) which have large surface area, tunable pore size and good thermal/chemical stability have been applied as efficient enzyme immobilization matrix [28,29] for fabrication of enzyme electrochemical biosensors for detection of methyl parathion [8], hydrogen peroxide [30] and bisphenol A [31]. MOFs particularly those with mesopores are able to encapsulate enzymes into their mesopores and eliminated the problem of enzymes aggregation and leaching [32,33]. It can also selectively accumulate target analytes to enhance specificity of the enzymatic reaction [30,34,35].

We have previously synthesized a type of MOF nanofibers which demonstrated good electrochemical behavior, excellent chemical and thermal stability; and high porosity and surface area [36]. Present study takes advantage of the unique microstructure and chemical property of MOF nanofibers; and employs it for fabrication of *burkholderia cepacia* lipase (BCL)@MOF nanofibers biosensor to detect methyl parathion residues in vegetables. Chitosan which is a cationic polysaccharide formed by monosaccharide chains linked by glycosidic bonds with polymer amino groups was used as a film forming agent to adhere BCL@MOF nanofibers to glassy carbon electrode. It is one of the most commonly used film forming agent in enzyme biosensors [37–39]. One of the uniqueness of our fabricated biosensor is it selectively catalyzes hydrolysis of methyl parathion to *p*-nitrophenol (PNP) and directly measures the redox current of the released PNP (Fig. 1A). Fabrication procedure of the BCL@MOF nanofibers biosensor was optimized and the performance of the biosensor in detecting a model pesticides (*p*-nitrophenyl palmitate, PNPP) was evaluated (Fig. 1B). The fabricated BCL@MOF nanofibers biosensor which is simple-to-be prepared demonstrated improved methyl parathion detection including wide linear range, low limit of detection, high selectivity and good stability.

2. Materials and methods

2.1. Materials

Copper (II) nitrate hexahydrate [$Cu(NO_3)_2.6H_2O$], L-aspartic acid and lipase from *Burkholderia cepacia* (BCL) were purchased from Sigma Aldrich. Chitosan (deacetylation 95%), *p*-nitrophenyl palmitate (PNPP), acetic acid and methyl parathion dissolved in methanol (1 mg mL^{-1}) were obtained from Aladdin. Other reagents including sodium hydroxide, potassium ferricyanide ($K_3[Fe(CN)_6]$), potassium ferrocyanide trihydrate ($K_4[Fe(CN_6)].3H_2O$) and sulfuric acid were obtained from Sinoreagent, China. Phosphate buffer solutions (PBS, 0.1 M, pH = 7.0) was prepared from potassium dihydrogen phosphate (0.75 M) and disodium hydrogen phosphate (0.25 M).

2.2. Synthesis and characterization of MOF nanofibers

MOF nanofibers were synthesized and characterized according to our previously reported method [36]. Briefly, an aqueous solution of Cu $(NO_3)_2.6H_2O$ (0.061 M, 6 mL) was mixed with 30 mL aqueous solution containing NaOH (0.1 M) and aspartic acid (0.5 M) at room temperature. The resulting deep blue solution was washed six times with distilled water and ethanol solution (1:1) MOF nanofibers were obtained by centrifugation and vacuum dried at 80 °C for 10 h. The as-prepared MOF nanofibers were characterized using scanning electron microscopy (SEM) and X-ray diffraction (XRD). XRD analysis were conducted using Bruker D8 Discover XRD (Cu radiation, λ = l.540596 Å) over the 2θ range of 5–50° at room temperature. Morphology of the MOF nanofibers was observed and imaged by SEM under a working potential of 3 kV with magnifications ranging from 7.35 to 44.87 K through using a focused ion beam scanning electron microscope (Carl Zeiss). Thermal

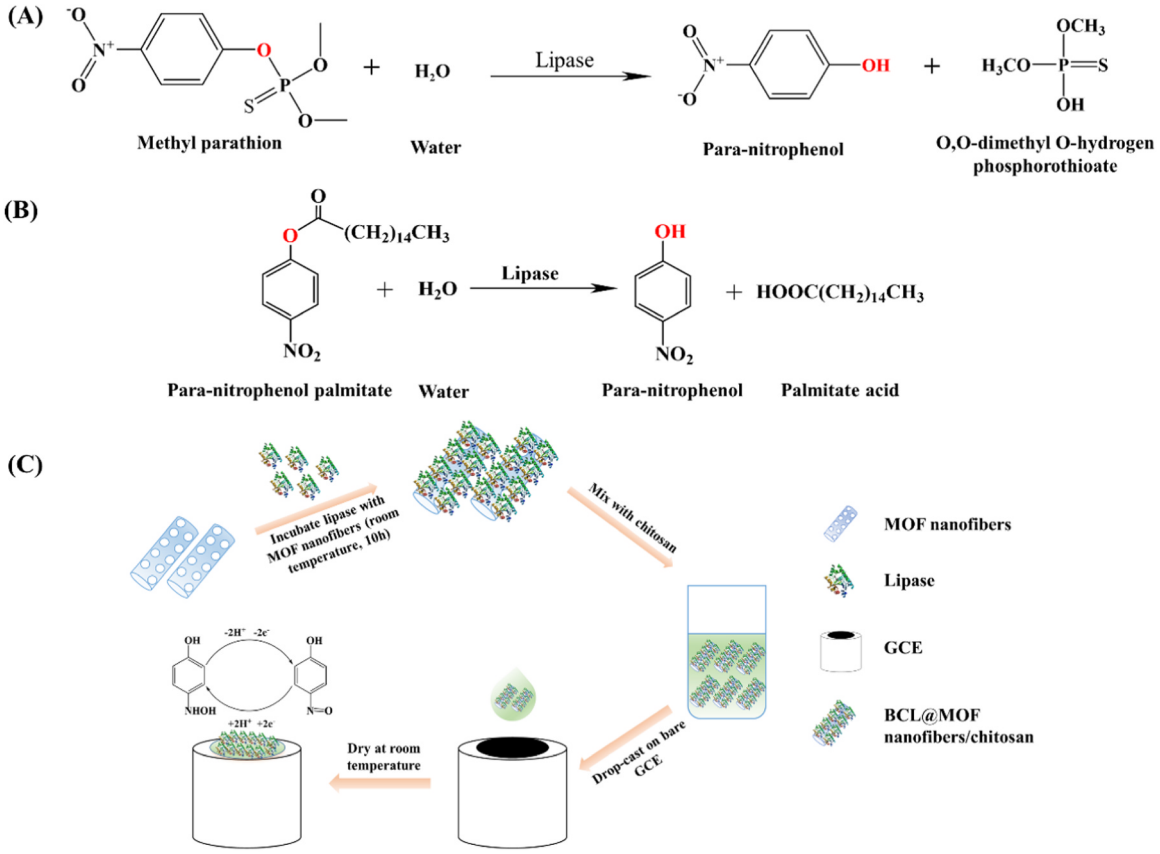

Fig. 1. (A) Lipase catalyzed hydrolysis of methyl parathion to *p*-nitrophenol; (B) Lipase catalyzed hydrolysis of *p*-nitrophenyl palmitate to *p*-nitrophenol (C); Fabrication procedures of BCL@MOF nanofibers/chitosan/GCE biosensor.

stability and porosity of the MOF nanofibers were evaluated using thermogravimetric analysis (Perkin–Elmer, Pyris Diamond TG/DTA) and nitrogen adsorption–desorption techniques (Micro-meritics, ASAP 2020 M), respectively.

2.3. Fabrication of the BCL@MOF nanofibers/chitosan/GCE biosensor

Fig. 1C shows fabrication of the BCL@MOF nanofibers/chitosan/GCE biosensor. GCE electrodes (3 mm) were firstly polished using Al_2O_3 powder (1.0, 0.3, 0.05 μM), cleaned in ethanol and water for three times, and finally dried under gentle N_2 stream. 100 μL of BCL solution [30 mg mL^{-1} PBS (0.1 M)] and 300 μL of MOF nanofibers aqueous solution (1 mg mL^{-1}) were mixed at 200 rpm for 10 h at room temperature. Following that, 100 μL of chitosan solution (6 mg mL^{-1}) was added to the mixture and vibrated for 3 min 5 μL of the resultant BCL@MOF nanofibers/chitosan was drop cast onto the surface of a freshly polished GCE. The prepared electrodes (BCL@MOF nanofibers/chitosan/GCE) were dried at room temperature and finally stored in 0.05 M PBS (pH 7.0) at 4 °C prior to usage.

2.4. Electrochemical measurements and sensing performance of the BCL@MOF nanofibers/chitosan/GCE biosensor

All electrochemical measurements were conducted using CHI760E electrochemical workstation (Chenhua, Shanghai) which is connected to a computer for data collection and analysis. A conventional three electrode system was employed with glassy carbon electrode (GCE) as working electrode, calomel electrode (internal solution: saturated potassium chloride) as reference electrode and platinum wire as auxiliary electrode. Electrochemical impedance spectroscopy (EIS) was conducted in N_2-saturated 0.1 M KCl solution containing 5.0 mM $Fe(CN)_6^{3-/4-}$ at open circuit potential in the frequency range from 0.01 to 10^5 Hz with the amplitude 5 mV. EIS data were analyzed using ZVIEW software. Cyclic voltammograms (CVs) were carried out in N_2-saturated 0.1 M PBS (pH 7.0) in the presence of 750 μM PNPP at a scanning rate of 50 mV s^{-1}. Differential pulse voltammetry (DPV) was performed in N_2-saturated 0.1 M PBS (pH 7.0) containing 10 μM methyl parathion (dissolved in methanol) with amplitude of 5 mV and pulse width of 0.2 s after five times of CV at a scanning rate of 50 mV s^{-1} ranging from 0.8 to −0.8 V. Electrochemical measurements were carried out in ambient environment.

LOD was determined according to the following equation:

$$LOD = 3SD/K$$

whereby SD refers to the standard deviation of the control measurement and K refers to slope of the calibration curve.

Storage stability of the BCL@MOF nanofibers/chitosan/GCE was evaluated by monitoring DPVs in 10 μM methyl parathion (dissolved in methanol). BCL@MOF nanofibers/chitosan/GCE was used for repeated methyl parathion detection during the storage period (0.05 M PBS pH 7.0 at 4 °C for 21 days).

2.5. Selectivity of the BCL@MOF nanofibers/chitosan/GCE biosensor

Selectivity of the BCL@MOF nanofibers/chitosan/GCE biosensor was carried by measuring CVs and DPVs of some potentially interfering substances such as dimethoate, diazinon, glucose, ascorbic acid, uric acid and benzoate (5 μM) in 0.1 M PBS (pH 7.0).

2.6. Electrochemical biosensing of methyl parathion residues in vegetables

Vegetable samples (lettuce and cabbage) were purchased from a local market in Ningbo, China. The vegetable samples were cleaned with distilled water and chopped into fine pieces. One grams of each chopped sample were spiked with 50 μL of methyl parathion solutions at different concentrations (0.10 μM, 0.15 μM and 0.20 μM). The spiked vegetable samples were then immersed in 5 mL methanol for 1 h at room temperature. Following that, vegetables were removed from the methanol solutions by filtration. The obtained methanol solutions were concentrated to 50 μL under gentle N_2 stream and mixed with 5 mL of PBS (pH 7.0) and used in DPV measurement.

3. Results and discussion

3.1. Characterization of the synthesized MOF nanofibers and BCL@MOF nanofibers

Characteristics of the MOF nanofibers have been reported in our previous findings [36]. Briefly, MOF nanofibers shows strong peaks at 2θ = 5.71, 10.93, 14.85, 19.88, 14.75, 26.32 and 28.65° indicating high crystallinity of the nanofibers. Both MOF nanofibers and BCL@MOF nanofibers possess homogenous fiber structures with a fiber diameter ranging from 100 nm to 200 nm and a fiber length of several microns. MOF nanofibers demonstrated thermal stability with no apparent weight loss at a temperature below 200 °C. In terms of pore size distribution, MOF nanofibers demonstrated a peak at 7.66 Å. The as-prepared MOF nanofibers possessed a Brunauer-Emmett-Teller (BET) surface area of 41.33 m^2 g^{-1} [36]. In addition, MOF nanofibers had a pore volume of 0.157 cm^2 g^{-1}. Following BCL immobilization, BCL@MOF nanofibers and BCL@MOF nanofibers/chitosan demonstrated reduced pore volume of 0.113 cm^2 g^{-1} and 0.063 cm^2 g^{-1}, respectively. This indicated successful immobilization of BCL into the pores of MOF nanofibers.

3.2. Electrochemical behavior of BCL@MOF nanofibers/chitosan/GCE

Fig. 2A shows CVs of bare GCE and BCL@MOF nanofibers/chitosan/GCE in 0.1 M N_2-saturated PBS (pH 7.0) containing 10 μM methyl parathion. In comparison to bare GCE, BCL@MOF nanofibers/chitosan/GCE demonstrated obvious redox peaks at ca. −0.108 and −0.236 V. PNP liberated from the lipase catalyzed hydrolysis of methyl parathion has been previously reported to participate in an irreversible reduction process to form 4-(hydroxyamino)phenol which can then be oxidized to form 4-nitrosophenol [40–42]. Redox peaks in present work can be attributed to the reversible redox process of 4-(hydroxyamino)phenol to 4-nitrosophenol [23,41,43].

Fig. 2B shows the redox peaks of BCL@MOF nanofibers/chitosan/GCE increased linearly with scan rate (30 mV s^{-1} to 250 mV s^{-1}) indicating a quasi-reversible surface process. According to the Laviron's theory of quasi-reversible thin-layer electrochemistry, electron transfer number (n) and electron transfer coefficient (α) could be obtained based on the following equations:

$$E_{pc} = E^{0'} - (2.3RT/\alpha nF)\log \nu \quad (1)$$

$$E_{pa} = E^{0'} - [2.3RT/(1-\alpha)nF]\log \nu \quad (2)$$

The n and α value of BCL@MOF nanofibers-based biosensor was 0.367 and 4.978, respectively. This indicated that only two electrons transfer was involved in the aforementioned electrochemical process (Fig. 2A).

3.3. Electrochemical impedance spectroscopy (EIS) of BCL@MOF nanofibers/ chitosan/GCE

Electron transfer properties and impedance changes of the BCL@MOF nanofibers/chitosan/GCE were investigated using EIS technique with $Fe(CN)_6^{3-/4-}$ as redox probe. Fig. 2C shows the Nyquist plots of bare GCE, chitosan/GCE, BCL@chitosan/GCE, MOF nanofibers/chitosan/GCE and BCL@MOF nanofibers/chitosan/GCE. Diameter of the semicircle at higher frequencies of the Nyquist plots corresponds to the electron transfer limited process and can be used as indicator of the electron transfer resistance (Rct). Rct of the different electrodes

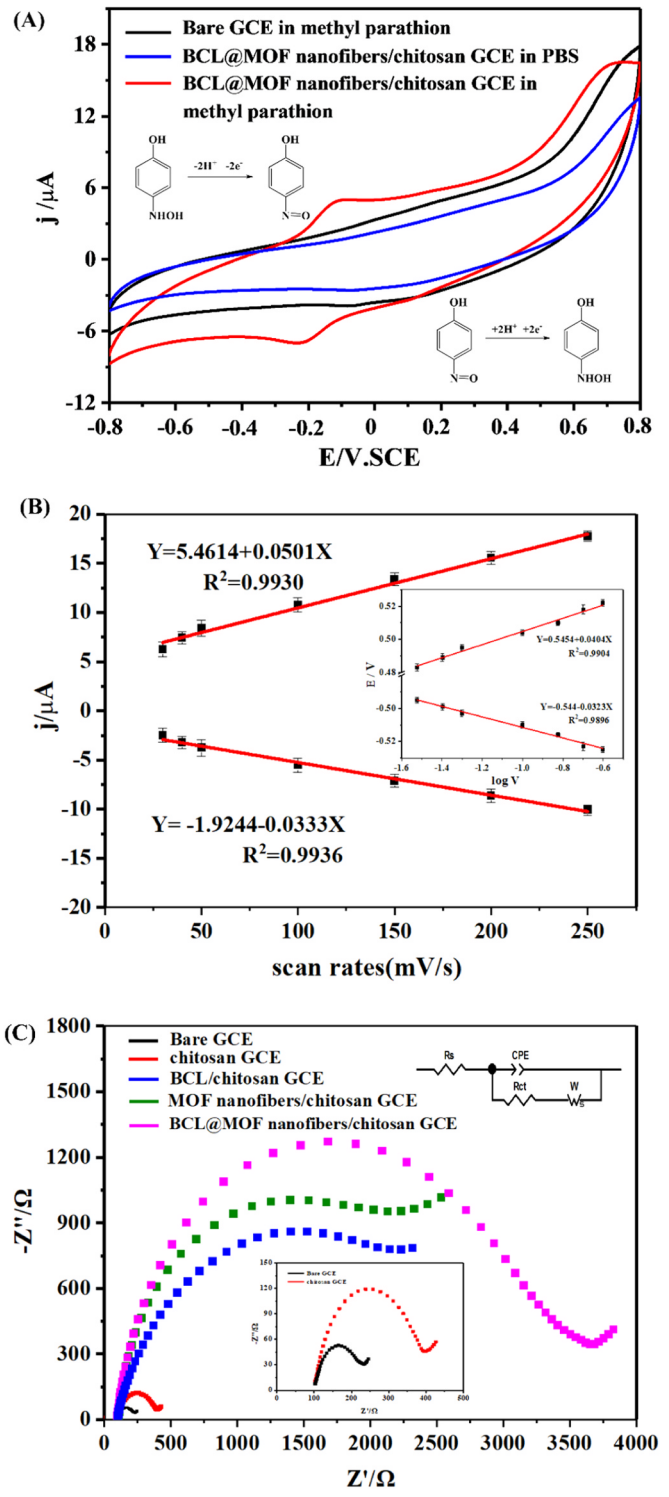

Fig. 2. (A) CV curve of bare GCE and BCL@MOF nanofibers/chitosan/GCE cycled in N_2-saturated 0.1 M PBS (pH 7.0) and N_2-saturated 0.1 M PBS (pH 7.0) containing 10 μM methyl parathion (potential window: −0.8–0.8 V vs. SCE at a scanning rate of 50 mV s^{-1}); (B) Plots of anodic peak potential and cathodic peak potential for BCL@MOF nanofibers electrode versus the logarithm of scan rate. (C) EIS of various electrodes in 0.1 M KCL aqueous solution containing 5 mM $[Fe(CN)_6]^{3-/4-}$:GCE electrode (black curve), chitosan/GCE electrode (red curve), BCL/chitosan/GCE electrode (blue curve), MOF nanofibers/chitosan/GCE electrode (olive curve), BCL@MOF nanofibers/chitosan/GCE electrode (magenta curve). (For interpretation of the references to color in this figure legend, the reader is referred to the web version of this article).

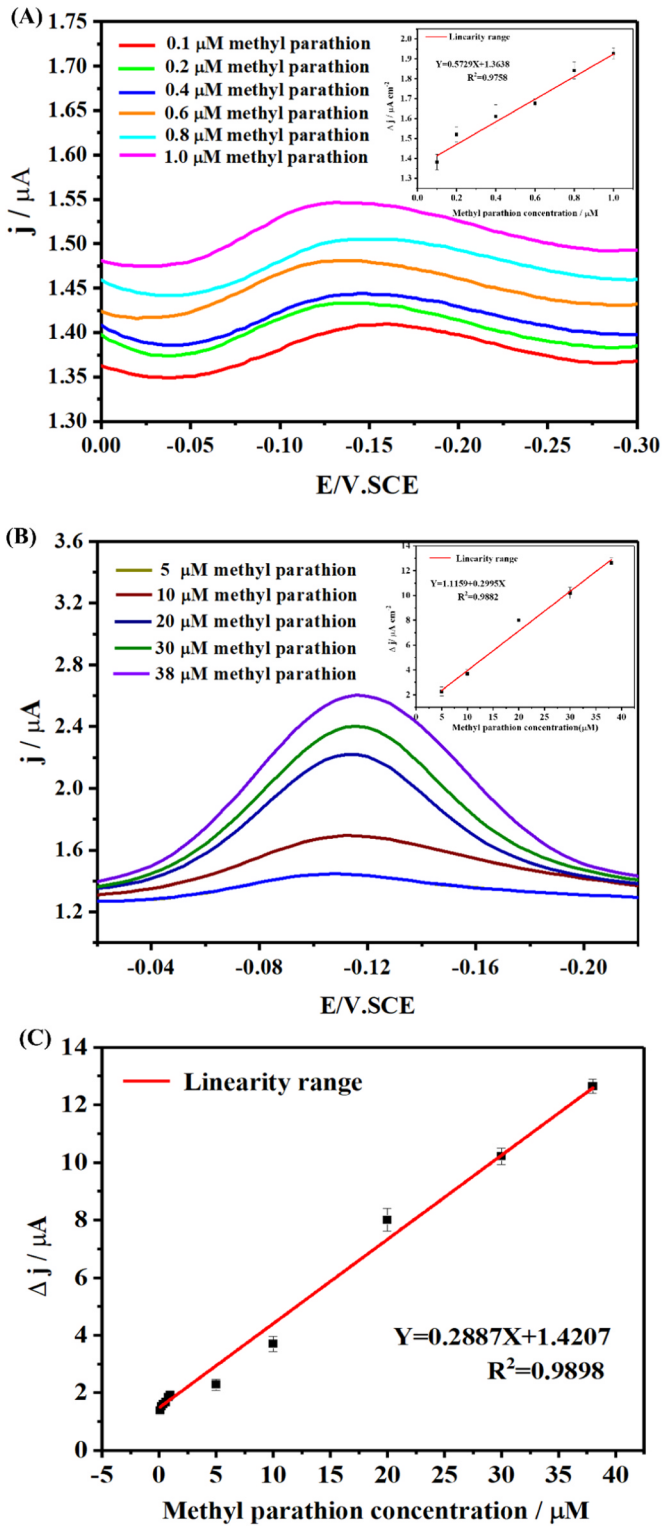

Fig. 3. (A) DPV of BCL@MOF nanofibers/chitosan/GCE electrode at 0.1–1.0 μM methyl parathion (inset : Delta current of BCL@MOF nanofibers/chitosan/GCE electrode at 0.1–1.0 μM methyl parathion). (B) DPV of BCL@MOF nanofibers/chitosan/GCE electrode at 5.0–38.0 μM methyl parathion (inset : Delta current of BCL@MOF nanofibers/chitosan/GCE electrode at 5.0–38.0 μM). (C) Linear curve of BCL@MOF nanofibers/chitosan/GCE electrode at 0.1–38.0 μM of methyl parathion.

Table 1
Comparison of the performance of BCL@MOF nanofibers/chitosan/GCE fabricated in present work with other published electrodes for methyl parathion determination.

Methods	Detection mechanism	Linear range	LOD	Reference
BCL@MOF nanofibers/chitosan/GCE	Direct	0.1–38 μM	0.067 μM	Present work
Lipase@ZIF-8 nanoparticles GCE	Direct	0.1–38 μM	0.28 μM	[8]
Lipase@Functionalized gold electrode	Direct	0.1–40 μM	0.1 μM	[9]
Lipase mobilized CPE	Direct	10–70 μM	26.32 μM	[10]
Colloidal TA@AuNPs GCE	Direct	0.03–167.7 μM	0.010 μM	[11]
NiO-SPEs platform	Direct	0.1–30 μM	0.024 μM	[12]
NCDs-MPH system	Direct	2.38–73.78 μM	0.338 μM	[13]

*BCL: *Burkholderia cepacia* Lipase; GCE: Glassy carbon electrodes; CPE: Carbon paste electrode; TA@AuNPs: Tannic acid@gold nanoparticles; NiO-SPEs: NiO Screen-printed electrodes; NCD-MPH: N-doped carbon dots and methyl parathion hydrolase.

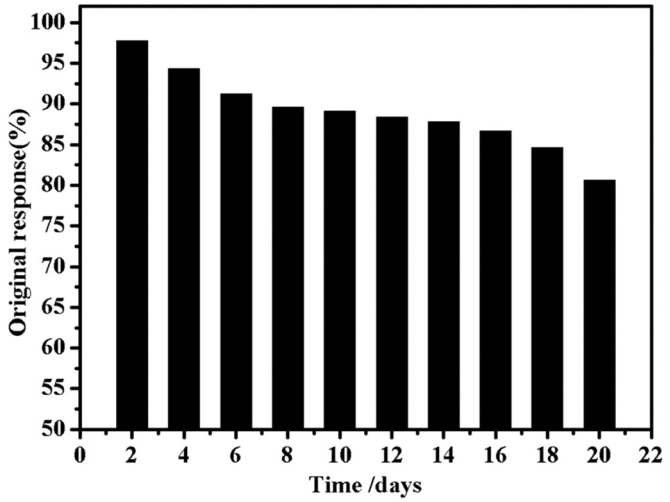

Fig. 4. DPV response of BCL@MOF nanofibers/chitosan/GCE electrode during storage in 0.05 M PBS at 4 °C for 21 days.

increases in the following order: bare GCE (232 Ω) < chitosan/GCE (396 Ω) < BCL@chitosan/GCE (2232 Ω) < MOF nanofibers/chitosan/GCE (2331 Ω) < BCL@MOF nanofibers/chitosan/GCE (3654 Ω). Bare GCE presents a small Rct value indicating a diffusion limiting process. A much higher Rct value can be observed following modification of the bare GCE surface with BCL@MOF nanofibers/chitosan indicating successful immobilization of the lipase onto GCE surface. Increased in the Rct value is mainly caused by steric hindrance, electrostatic interactions and partial blockage of interfacial electrons by lipase molecules which has poor conductivity [2].

3.4. Electrochemical detection of methyl parathion by BCL@MOF nanofibers/ chitosan/GCE

Methyl parathion can be easily detected using DPV on the BCL@MOF nanofibers/chitosan/GCE. Lipase concentration and dropping volume of BCL@MOF nanofibers onto bare GCE were optimized for detection of methyl parathion. Current responses of the BCL@MOF nanofibers/chitosan/GCE was found to increase with both lipase concentration and dropping volume. Increased in BCL concentration from 5 to 30 mg mL^{-1} resulted in increased in current responses of the BCL@MOF nanofibers/chitosan/GCE from 4.125 μA cm^{-2} to 6.721 μA cm^{-2} (Fig. S1A). Meanwhile, increased in dropping volume of BCL@MOF nanofibers onto GCE from 3 to 5 μL also resulted in increased in current responses of the BCL@MOF nanofibers /chitosan/GCE from 3.960 μA cm^{-2} to 5.565 μA cm^{-2} (Fig. S1B). Finally, a BCL concentration of 30 mg mL^{-1} and a dropping volume of 5 μL were used for fabrication of biosensors used in subsequent analysis.

Relationship between DPV response and methyl parathion concentration evaluated. Fig. 3 shows BCL@MOF nanofibers/chitosan/GCE demonstrated linearity at wide methyl parathion concentration (0.1–38 μM MP) with a linear regression equation of $Y = 0.2887 \times (\pm 0.00112) + 1.4207 (\pm 0.01272)$ ($R^2 = 0.9898$). The lower limit of detection for methyl parathion by BCL@MOF nanofibers/chitosan/GCE biosensor was 0.067 μM.

Sensing performance of the as-prepared BCL@MOF nanofibers/chitosan/GCE were found to be comparably better than those currently reported electrochemical biosensor for direct detection of pesticides (Table 1). To our knowledge, limited study has been conducted to apply MOF as immobilization matrix in fabrication of electrochemical biosensor for direct detection of methyl parathion. We have previously used rhombic dodecahedron ZIF-8 nanoparticles as immobilization matrix in lipase-based electrochemical biosensors to detect methyl parathion [8]. Although MOF nanofibers synthesized in present study had a lower BET surface area than ZIF-8 nanoparticles, present study found that BCL@MOF nanofibers/chitosan/GCE demonstrated a much lower detection limit indicating high sensitivity of the MOF nanofibers-based biosensor. One of the possible reasons is ability of CuO in the MOF nanofiber to participate in the redox process of the PNP. PNP can be oxidized to a mesomeric phenoxonium ion which participated in a C-C coupling reaction with another PNP to produce a dimer [8,44].

3.5. Reusability and stability of the BCL@MOF nanofibers/chitosan/GCE

Unlike the single-use acetylcholinesterase and organophosphorus hydrolase biosensors, the as-prepared BCL@MOF nanofibers/chitosan/GCE have great reusability and excellent stability. Fig. 4 shows the as-prepared BCL@MOF nanofibers/chitosan/GCE can be reused for at least 20 days when stored in 0.05 M PBS (pH = 7) at 4 °C. Only slight decreased in current response was observed during the first 10 days with retainment of 90% of its initial response. Furthermore, the BCL@MOF nanofibers/chitosan/GCE can retain at least 80% of its initial response to methyl parathion after three weeks storage. Decreased in the current response might be attributed to the leaching of the immobilized lipase. Nevertheless, it is evident that the BCL@MOF nanofibers/chitosan/GCE have good reusability and excellent stability for detection of methyl parathion during storage period up to 3 weeks.

3.6. Selectivity of the BCL@MOF nanofibers/chitosan/GCE biosensor

Selectivity of the BCL@MOF nanofibers/chitosan/GCE biosensor was evaluated against other pesticides (dimethoate and diazinon) and possible interfering substances including glucose, ascorbic acid, uric acid and benzoate. Fig. 5A-B shows no or low CV and DPV signals can be detected from the aforementioned potentially interfering substances indicating good selectivity of the biosensors in detection of methyl parathion. A plot of ratio of interference DPV to methyl parathion DPV shows a highest value of 8.72% (dimethoate), which indicates that all the studied interfering substances do not interfere with determination of methyl parathion (Fig. 5C).

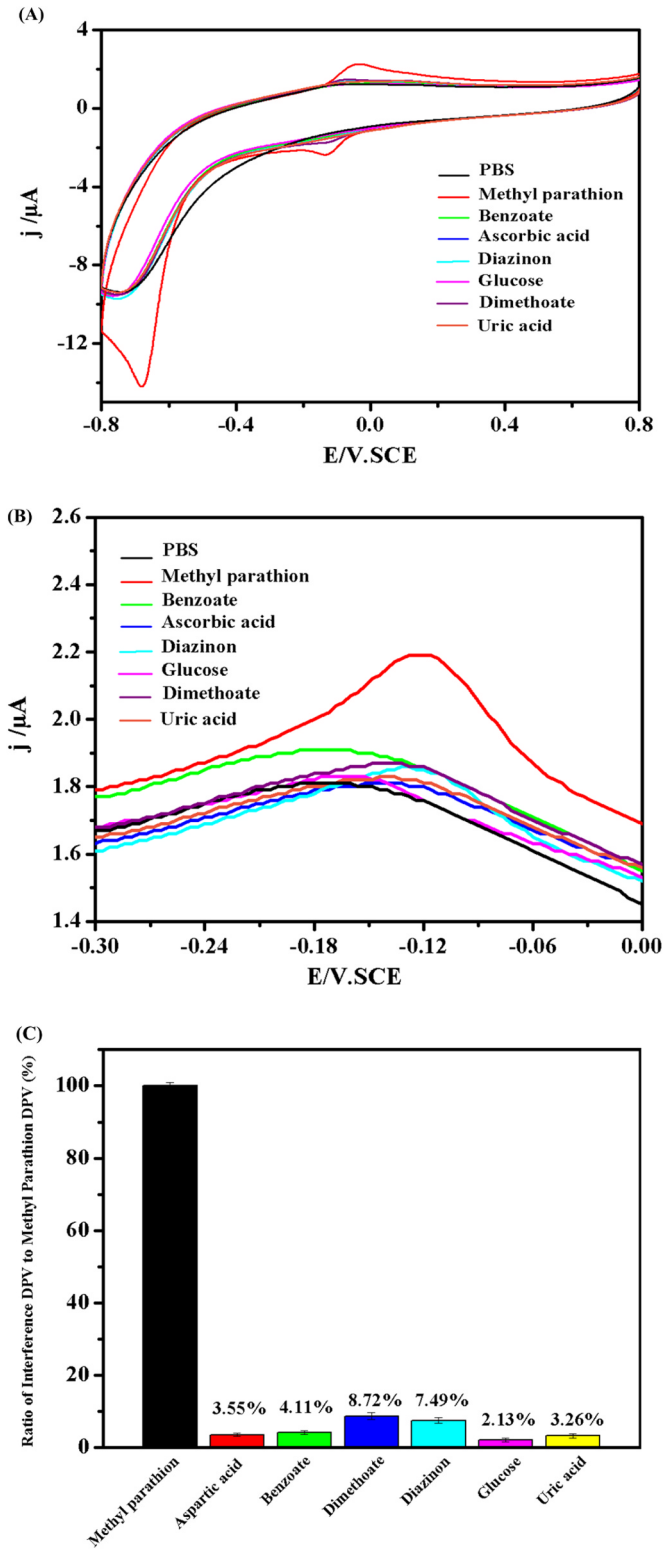

Fig. 5. (A) CV curve of BCL@MOF nanofibers/chitosan/GCE cycled in N_2-saturated 0.1 M PBS (pH 7.0) containing 5 μM of methyl parathion, dimethoate, diazinon, glucose, ascorbic acid, uric acid or benzoate (potential window: −0.8–0.8 V vs. SCE at a scanning rate of 50 mV s^{-1}); (B) DPV response of BCL@MOF nanofibers/chitosan/GCE electrode at 5 μM of methyl parathion, dimethoate, diazinon, glucose, ascorbic acid, uric acid or benzoate; (C) Ratio of interfering substances DPV to ratio of methyl parathion DPV measured by BCL@MOF nanofibers/chitosan/GCE.

Table 2
Determination of methyl parathion residues in vegetable samples by BCL@MOF nanofibers/chitosan/GCE.

Materials	Added(μg)	Found(μg)	Recovery(%)	RSD(%)
Lettuce	26.321	25.058	95.2	6.94
	39.482	41.59	105.34	4.45
	52.642	51.282	93.85	5.52
Cabbage	26.321	28.085	106.71	6.3
	39.482	37.765	95.65	5.3
	52.642	44.814	85.13	1.0

3.7. Application of the BCL@MOF nanofibers/chitosan/GCE for detection of methyl parathion in vegetable samples

Chinese national standard clearly stipulated that the maximum allowable limit of methyl parathion in food shall not exceed 0.02 mg kg^{-1} [45]. We have evaluated the biosensing performance of the as prepared BCL@MOF nanofibers/chitosan/GCE in detecting methyl parathion residues in two vegetable samples namely lettuce and cabbage. As no methyl parathion residues were detected in both vegetable samples, we have spiked the samples with different concentrations of methyl parathion (26.321 μg g^{-1}, 39.482 μg g^{-1}, 52.642 μg g^{-1}). Recoveries of spiked methyl parathion in both lettuce and cabbage samples were observed in the range from 85 ± 1–107 ± 6% indicating good reliability of the as prepared biosensors (Table 2).

4. Conclusions

A novel simple-to-prepare BCL@MOF-nanofibers/chitosan/GCE biosensor was successfully developed for rapid and sensitive detection of methyl parathion in vegetable samples. MOF-nanofibers with possesses large surface area was shown to be a suitable matrix for immobilization of BCL with the problem of enzyme leaching and aggregation. Under the optimal operating conditions, the BCL@MOF nanofibers /chitosan/GCE biosensor demonstrated high sensitivity for methyl parathion detection with a wide linear range (0.1–38 μM) and low limit of detection (0.067 μM). The BCL@MOF nanofibers/chitosan/GCE biosensor also have good reusability and excellent stability for detection of MP during storage period up to 3 weeks with retainment of more than least 80% of its initial response. When applied for detection of methyl parathion residues in vegetable samples, the BCL@MOF nanofibers/chitosan/GCE biosensor demonstrated good recovery rates.

Acknowledgements

This work was sponsored by K.C. Wong Magna Fund in Ningbo University. Ling-Zhi Cheong acknowledged funding support from Ningbo University (421401560) and National Natural Science Foundation of China (21706137).

Funding Information

This work was sponsored by K.C. Wong Magna Fund in Ningbo University. Ling-Zhi Cheong acknowledged funding support from National Natural Science Foundation of China (21706137), Ningbo University (421401560) and Key Laboratory of Animal Protein Food Deep Processing Technology of Zhejiang Province (421600240).

Appendix A. Supporting information

Supplementary data associated with this article can be found in the online version at doi:10.1016/j.talanta.2019.01.052.

References

[1] P. Carullo, G.P. Cetrangolo, L. Mandrich, G. Manco, F. Febbraio, Fluorescence spectroscopy approaches for the development of a real-time organophosphate detection system using an enzymatic sensor, Sensors 15 (2) (2015) 3932–3951.

[2] J. Bao, C. Hou, Q. Dong, X. Ma, J. Chen, D. Huo, M. Yang, K.H.A.E. Galil, W. Chen, Y. Lei, ELP-OPH/BSA/TiO2 nanofibers/c-MWCNTs based biosensor for sensitive and selective determination of p-nitrophenyl substituted organophosphate pesticides in aqueous system, Biosens. Bioelectron. 85 (Supplement C) (2016) 935–942.

[3] H.-F. Cui, W.-W. Wu, M.-M. Li, X. Song, Y. Lv, T.-T. Zhang, A highly stable acetylcholinesterase biosensor based on chitosan-TiO2-graphene nanocomposites for detection of organophosphate pesticides, Biosens. Bioelectron. 99 (2018) 223–229.

[4] P. Kumar, K.-H. Kim, A. Deep, Recent advancements in sensing techniques based on functional materials for organophosphate pesticides, Biosens. Bioelectron. 70 (2015) 469–481.

[5] W. Zhu, W. Liu, T. Li, X. Yue, T. Liu, W. Zhang, S. Yu, D. Zhang, J. Wang, Facile green synthesis of graphene-Au nanorod nanoassembly for on-line extraction and sensitive stripping analysis of methyl parathion, Electrochim. Acta 146 (2014) 419–428.

[6] D. Pan, S. Ma, X. Bo, L. Guo, Electrochemical behavior of methyl parathionand its sensitive determination at a glassycarbon electrode modified with order-edmesoporous carbon, Microchim. Acta 173 (2011) 215–221.

[7] P.R. de Oliveira, C. Kalinke, J.L. Gogola, A.S. Mangrich, L.H.M. Junior, M.F. Bergamini, The use of activated biochar for development of a sensitive electrochemical sensor for determination of methyl parathion, J. Electroanal. Chem. 799 (2017) 602–608.

[8] B. Ma, L.-Z. Cheong, X. Weng, C.-P. Tan, C. Shen, Lipase@ZIF-8 nanoparticles-based biosensor for direct and sensitive detection of methyl parathion, Electrochim. Acta 283 (2018) 509–516.

[9] N. Zehani, S.V. Dzyadevych, R. Kherrat, N.J. Jaffrezic-Renault, Sensitive impedimetric biosensor for direct detection of diazinon based on lipases, Front. Chem. 2 (2014).

[10] K.G. Reddy, G. Madhavi, B.E.K. Swamy, S. Reddy, A.V.B. Reddy, V. Madhavi, Electrochemical investigations of lipase enzyme activity inhibition by methyl parathion pesticide: voltammetric studies, J. Mol. Liq. 180 (2013) 26–30.

[11] P. Balasubramanian, T.S.T. Balamurugan, S.-M. Chen, T.-W. Chen, G. Sharmila, M.-C. Yu, One-step green synthesis of colloidal gold nano particles: a potential electrocatalyst towards high sensitive electrochemical detection of methyl parathion in food samples, J. Taiwan Inst. Chem. Eng. 87 (2018) 83–90.

[12] M. Khairy, H.A. Ayoub, C.E. Banks, Non-enzymatic electrochemical platform for parathion pesticide sensing based on nanometer-sized nickel oxide modified screen-printed electrodes, Food Chem. 255 (2018) 104–111.

[13] W. Song, H.-J. Zhang, Y.-H. Liu, C.-L. Ren, H.-L. Chen, A new fluorescence probing strategy for the detection of parathion-methyl based on N -doped carbon dots and methyl parathion hydrolase, Chin. Chem. Lett. 28 (8) (2017) 1675–1680.

[14] M. Wei, G. Zeng, Q. Lu, Determination of organophosphate pesticides using an acetylcholinesterase-based biosensor based on a boron-doped diamond electrode modified with gold nanoparticles and carbon spheres, Microchim. Acta 181 (1-2) (2013) 121–127.

[15] K.-E. Jaeger, T. Eggert, Lipases for biotechnology, Curr. Opin. Biotechnol. 13 (4) (2002) 390–397.

[16] A. Schmid, J.S. Dordick, B. Hauer, A. Kiener, M. Wubbolts, B. Witholt, Industrial biocatalysis today and tomorrow, Nature 409 (2001) 258–268.

[17] R. Wohlgemuth, Biocatalysis—key to sustainable industrial chemistry, Curr. Opin. Biotechnol. 21 (6) (2010) 713–724.

[18] C. Wu, X. Liu, Y. Li, X. Du, X. Wang, P. Xu, Lipase-nanoporous gold biocomposite modified electrode for reliable detection of triglycerides, Biosens. Bioelectron. 53 (2014) 26–30.

[19] K. Gangadhara Reddy, G. Madhavi, B.E. Kumara Swamy, Mobilized lipase enzymatic biosensor for the determination of chlorfenvinphos and malathion in contaminated water samples: a voltammetric study, J. Mol. Liq. 198 (2014) 181–186.

[20] N. Zehani, R. Kherrat, S.V. Dzyadevych, N. Jaffrezic-Renault, A microconductometric biosensor based on lipase extracted from Candida rugosa for direct and rapid detection of organophosphate pesticides, Int. J. Environ. Anal. Chem. 95 (5) (2015) 466–479.

[21] F. Febbraio, L. Merone, G.P. Cetrangolo, M. Rossi, R. Nucci, G. Manco, Thermostable esterase 2 from alicyclobacillus acidocaldarius as biosensor for the detection of organophosphate pesticides, Anal. Chem. 83 (5) (2011) 1530–1536.

[22] B. Tiwari, E. Verma, S. Chakraborty, A.K. Srivastava, A.K. Mishra, Tolerance strategies in cyanobacterium fischerella sp. under pesticide stress and possible role of a carbohydrate-binding protein in the metabolism of methyl parathion (MP), Int. Biodeterior. Biodegrad. 127 (2018) 217–226.

[23] N. Alvarenga, W.G. Birolli, E.B. Meira, S.C.O. Lucas, I.L. de Matos, M. Nitschke, L.P.C. Romão, A.L.M. Porto, Biotransformation and biodegradation of methyl parathion by Brazilian bacterial strains isolated from mangrove peat, Biocatal. Agric. Biotechnol. 13 (2018) 319–326.

[24] T. Loučka, M. Došek, S. Kříženecká, P. Janoš, Electrochemical behaviour and degradation of methyl parathion on platinum electrode, J. Electroanal. Chem. 823 (2018) 580–587.

[25] S. Pattanayak, S. Chakraborty, S. Biswas, D. Chattopadhyay, M. Chakraborty, Degradation of Methyl Parathion, a common pesticide and fluorescence quenching of Rhodamine B, a carcinogen using β- d glucan stabilized gold nanoparticles, J. Saudi Chem. Soc. (2018).

[26] S. Panky, K. Thandavan, D. Sivalingam, S. Sethuraman, U.M. Krishnan, B.G. Jeyaprakash, J.B.B. Rayappan, Lipase immobilized on nanostructured cerium oxide thin film coated on transparent conducting oxide electrode for butyrin sensing, Mater. Chem. Phys. 137 (3) (2013) 892–897.

[27] B. Tiwari, S. Chakraborty, A.K. Srivastava, A.K. Mishra, Biodegradation and rapid removal of methyl parathion by the paddy field cyanobacterium fischerella sp, Algal Res. 25 (2017) 285–296.

[28] Z. Fan, J. Wang, Y. Nie, L. Ren, B. Liu, G. Liu, Metal-organic frameworks/graphene oxide composite: a new enzymatic immobilization carrier for hydrogen peroxide biosensors, J. Electrochem. Soc. 163 (3) (2016) B32–B37.

[29] Y. Wang, Y. Zhu, A. Binyam, M. Liu, Y. Wu, F. Li, Discovering the enzyme mimetic activity of metal-organic framework (MOF) for label-free and colorimetric sensing of biomolecules, Biosens. Bioelectron. 86 (2016) 432–438.

[30] W. Chen, W. Yang, Y. Lu, W. Zhu, X. Chen, Encapsulation of enzyme into mesoporous cages of metal-organic frameworks for the development of highly stable electrochemical biosensors, Anal. Methods 9 (21) (2017) 3213–3220.

[31] X. Wang, X. Lu, L. Wu, J. Chen, 3D metal-organic framework as highly efficient biosensing platform for ultrasensitive and rapid detection of bisphenol A, Biosens. Bioelectron. 65 (2015) 295–301.

[32] L.T. Liu, Y.L. Zhou, S. Liu, M.T. Xu, The applications of metal-organic frameworks in electrochemical sensors, ChemElectroChem 5 (1) (2018) 6–19.

[33] N. Bagheri, A. Khataee, B. Habibi, J. Hassanzadeh, Mimetic Ag nanoparticle/Zn-based MOF nanocomposite (AgNPs@ZnMOF) capped with molecularly imprinted polymer for the selective detection of patulin, Talanta 179 (2018) 710–718.

[34] L.-Z. Cheong, Y. Wei, H. Wang, Z. Wang, X. Su, C. Shen, Facile fabrication of a stable and recyclable lipase@amine-functionalized ZIF-8 nanoparticles for esters hydrolysis and transesterification, J. Nanopart. Res. 19 (8) (2017) 280.

[35] S.S. Nadar, V.K. Rathod, Encapsulation of lipase within metal-organic framework (MOF) with enhanced activity intensified under ultrasound, Enzym. Microb. Technol. 108 (2018) 11–20.

[36] C. Zhao, C. Shen, W. Han, Metal-organic nanofibers as anodes for lithium-ion batteries, RSC Adv. 5 (26) (2015) 20386–20389.

[37] M.C. Ribeiro, V.L.R. Correa, F.K.L. da Silva, J.R. de Oliveira Neto, A.A. Casas, L.B. de Menezes, A.C. Amaral, Improving peptide quantification in chitosan nanoparticles, Int J. Biol. Macromol. 119 (2018) 32–36.

[38] H.B.T. Moran, J.L. Turley, M. Andersson, E.C. Lavelle, Immunomodulatory properties of chitosan polymers, Biomaterials 184 (2018) 1–9.

[39] B. Krajewska, Application of chitin- and chitosan-based materials for enzyme immobilizations: a review, Enzym. Microb. Technol. 35 (2–3) (2004) 126–139.

[40] T. Alizadeh, M.R. Ganjali, P. Norouzi, M. Zare, A. Zeraatkar, A novel high selective and sensitive para-nitrophenol voltammetric sensor, based on a molecularly imprinted polymer–carbon paste electrode, Talanta 79 (5) (2009) 1197–1203.

[41] Z. Liu, J. Du, C. Qiu, L. Huang, H. Ma, D. Shen, Y. Ding, Electrochemical sensor for detection of p-nitrophenol based on nanoporous gold, Electrochem. Commun. 11 (7) (2009) 1365–1368.

[42] N. Chouhan, R. Ameta, R.K. Meena, Biogenic silver nanoparticles from Trachyspermum ammi (Ajwain) seeds extract for catalytic reduction of p -nitrophenol to p -aminophenol in excess of NaBH 4, J. Mol. Liq. 230 (2017) 74–84.

[43] A.H.A. Hassan, S.L. Moura, F.H.M. Ali, W.A. Moselhy, Md.P. Taboada Sotomayor, M.I. Pividori, Electrochemical sensing of methyl parathion on magnetic molecularly imprinted polymer, Biosens. Bioelectron. (2018).

[44] X. Tang, B. Zhang, Y. Li, Y. Xu, Q. Xin, W. Shen, CuO/CeO2 catalysts: redox features and catalytic behaviors, Appl. Catal. A: Gen. 288 (1) (2005) 116–125.

[45] N.H.a.F.P.C.o.t.P.R.o. China, National food safety standards, Maximum residue limits of pesticides in food, China and the People's Republic of China and the Ministry of Agriculture, 2016, pp. 90–91.